

# Statistical Long-Term Correlations in Dissociated Cortical Neuron Recordings

Federico Esposti, *Student Member, IEEE*, Maria G. Signorini, Steve M. Potter, and Sergio Cerutti, *Senior Member, IEEE*

**Abstract**—The study of nonlinear long-term correlations in neuronal signals is a central topic for advanced neural signal processing. In particular, the existence of long-term correlations in neural signals recorded via multielectrode array (MEA) could provide interesting information about changes in interneuron communications. In this study we propose a new method for long-term correlation analysis of neuronal burst activity based on the periodogram  $\alpha$  slope estimation of the MEA signal. We applied our method to recordings taken from cultured networks of dissociated rat cortical neurons. We show the effectiveness of the method in analyzing the activity changes as well as the temporal dynamics that take place during the development of such cultures. Results demonstrate that the  $\alpha$  parameter is able to divide the network development in three well-defined stages, showing pronounced variations in the long-term correlation among bursts.

**Index Terms**—Long-term correlations, multielectrode array (MEA), periodogram.

## I. INTRODUCTION

IN last decade the mammalian cortex has been deeply studied *in vitro* in the form of dissociated neuro-glial cultures implanted on multielectrode arrays (MEAs) [1]–[10]. One of the fundamental features of neuronal networks that is often investigated through MEA devices is “spontaneous activity” [11]–[13]. It refers to the activity that the network shows in absence of any external stimulation. It is well known that this behavior, also reported in *in vivo* studies, is characterized by periodic synchronization episodes, usually called bursts (as reported, e.g., in [14]–[17]). Moreover it was observed that both single electrode [18] and multielectrode [19]–[21] neuronal recordings exhibit nonlinear long-term characteristics [22].

The study of nonlinear long-term correlations in neuronal signals is a central topic for advanced MEA signal processing. In particular, the existence of long-term correlations (LTC) in such a signal could provide interesting information about changes in interneuron communications (e.g., LTP or LTD) correlated with the administration of neuroactive drugs or with the development of the network itself.

In this study we propose a method based on a calculation of  $\alpha$  coefficient in the power-law fitting of the experimental data

Manuscript received November 28, 2008; revised February 10, 2009; accepted March 23, 2009. First published May 27, 2009; current version published August 07, 2009.

F. Esposti, M. G. Signorini, and S. Cerutti are with the Dipartimento di Bioingegneria, Politecnico di Milano, 20133 Milano, Italy (e-mail: federico.esposti@polimi.it; mariagabriella.signorini@biomed.polimi.it; sergio.cerutti@polimi.it).

S. M. Potter is with the Department of Biomedical Engineering, Georgia Institute of Technology, Atlanta, GA 30332 USA (e-mail: steve.potter@bme.gatech.edu).

Digital Object Identifier 10.1109/TNSRE.2009.2022832

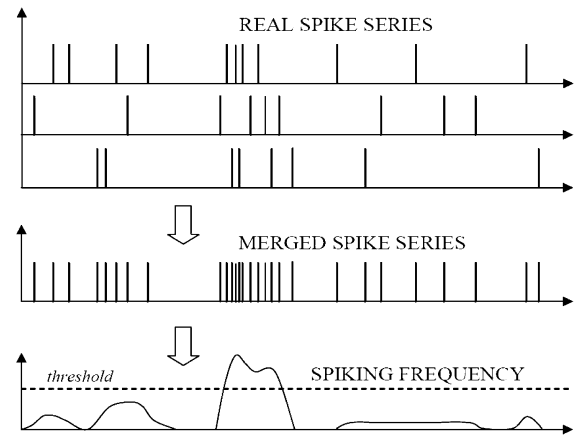


Fig. 1. Graphical representation of the burst detection algorithm (for simplicity three channels only are represented in figure).

in long-term correlation analysis of neuronal burst activity of dissociated cortical neurons studied through MEA recordings. Further, we study the changes in the LTC behavior induced by the network development.

## II. MATERIALS AND METHODS

### A. Cell Cultures, MEA Recordings, and Spike Sorting

In the present study we employed MEA data collected and described by Wagenaar *et al.* in [17]. In particular, we employed 12 30-min-long recordings classified as “dense” and 12 classified as “small” in [17]. In brief, these recordings were performed on cultures of E18 rat cortical neurons (plus glia) with a density of  $2.5 \pm 1.5 \cdot 10^3$  cells/mm<sup>2</sup> and  $1.6 \pm 0.6 \cdot 10^3$  cells/mm<sup>2</sup> at the first day *in vitro* (div), respectively, recorded longitudinally from the 6th to the 35th div with 59 electrode MEAs with a diameter of 30  $\mu$ m, purchased from Multi-Channel Systems (Reutlingen, Germany). The electrodes were organized in a square grid with the corners missing, spaced 200  $\mu$ m center-to-center. Spike sorting was performed with the MEABench software [23], using a threshold based detector. Spikes were detected as upward or downward excursions beyond  $4.5 \cdot$  (estimated rms noise), as described in [17]; in the same reference, details about dissections, cultures, recordings and spike detection, may be found.

### B. Analysis Procedure

As expected, the recordings showed spontaneous activity characterized by periodic synchronization episodes, usually called population bursts. In order to approach an intraburst

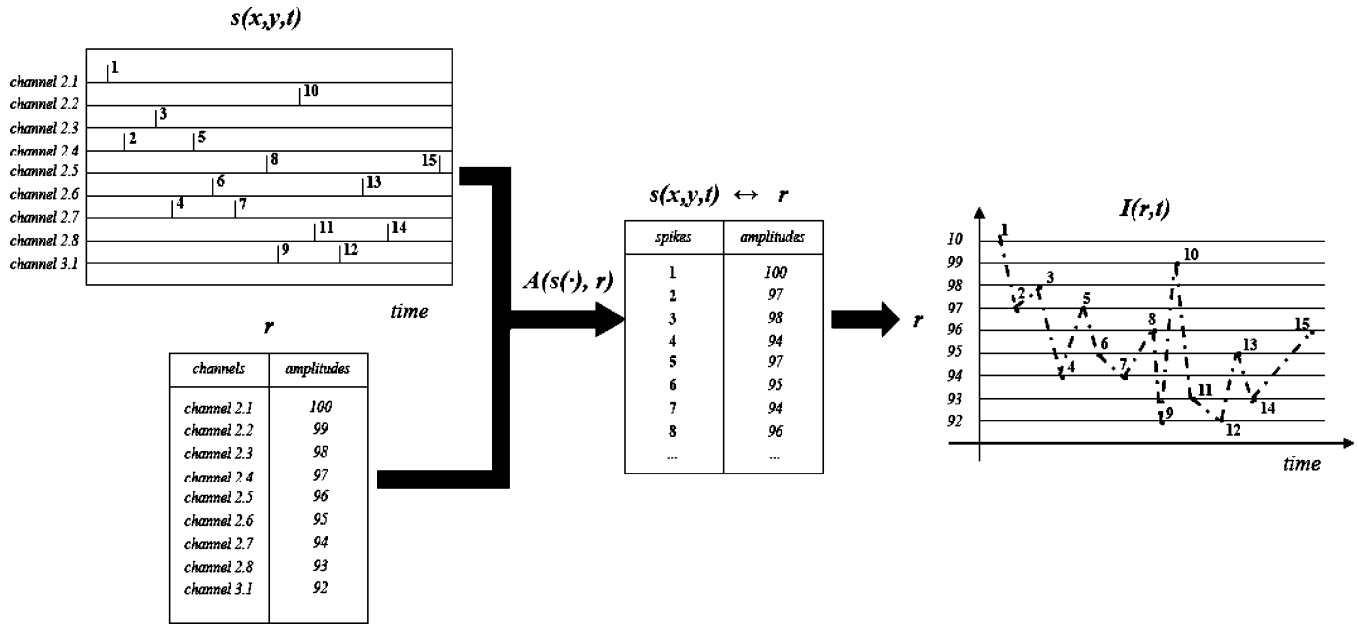


Fig. 2. Graphical example of the role of the arrangement algorithm  $r$  and the Space-Amplitude Transform method,  $A(s(\cdot), r)$ , at work with a nine channel raster plot. The transform joins together the raster plot,  $s(x, y, t)$ , and the arrangement vector,  $r$ , creating a lookup table in which to each spike is associated one amplitude value. The final output signal,  $I(r, t)$ , is obtained by merging the spatial/amplitude information deriving from the lookup table and the temporal information from the original raster plot.

analysis, we proposed and employed a frequency-based burst detector algorithm. Fig. 1 represents how the algorithm works: all MEA channels are merged forming a single series, showing on the  $x$  axis the recording time and on the  $y$  axis the spiking activity of all channels. Along this series the starting point of a burst is detected comparing the merged series with a frequency threshold fixed at 10 Hz. Frequency is computed as the inverse of the interspike interval (ISI) of the merged series. The reference duration of a burst is chosen to be 200 ms. Such parameters were chosen by training the algorithm on the experimental dataset. 10 Hz demonstrated as the most performing frequency threshold for the burst detection algorithm and 200 ms was the average maximal length of the burst we detected in the recordings.

Some controls are implemented in order to verify the presence of a real burst. First, the number of channels involved has to be more than the 15% of the total channel number. A channel is considered as “firing” if it spikes at least three times in the 200 ms time window. Moreover, two detected bursts can not be closer than 600 ms.

Thanks to the above procedure, we extracted the time-instants in which bursts took place in the recordings. The application of complex nonlinear signal processing methods for long-term correlation estimation requires one to work with 1-D data. As a matter of fact, most nonlinear signal processing methods are designed for 1-D data only. For this reason we processed MEA recordings (in particular, bursting epochs of the MEA raster plots, extracted thanks to the burst detection algorithm) in order to obtain 1-D signals. We applied the space amplitude transform (SAT), originally introduced in our paper [24], in order to perform such a conversion.

The space-amplitude transform,  $A(s(\cdot), r)$ , is a geometric transform that executes a projection from a 2-D domain set  $s(x, y, t)$ , e.g., the usual Raster plot, to a 1-D image set  $I(r, t)$ , exploiting an arrangement table  $r$  as Fig. 2 describes in detail.

In the domain set  $s(x, y, t)$ , i.e., in the Raster plot, a spike is coded in terms of 0 or 1 event. Each spike is characterized by spatiotemporal coordinates  $(x, y, t)$ :  $(x, y)$  correspond to a specific MEA channel and  $(t)$  identifies the time instant.

The  $A(s(\cdot), r)$  transform codes the MEA channels thanks to the arrangement table  $r$ , that is a “correspondence table” in which different amplitude values are univocally assigned to each channel of  $s(x, y, t)$ . In this way, an amplitude value corresponds to just one channel, and vice versa. The output of  $A(s(\cdot), r)$  is a lookup table in which an amplitude value is assigned to each spike of the raster plot, as function of the channel in which the spike takes place. Finally, a 1-D signal  $I(r, t)$  is created; this signal combines the amplitude information that derives from the above lookup table and the temporal information that is preserved from the starting raster plot  $s(x, y, t)$ .

The final output of the transformation,  $I(r, t)$ , is a representation of the spatial and temporal activity of the whole network (Fig. 3). In this process, no spatial or temporal information is lost with respect to the starting raster plot. The possibility to completely reconstruct the topological structure of the activity is granted by the biunivocal correspondence of the space-amplitude transform.

The method allows to approach an intrinsically 2-D plus time dataset, i.e., the time recording deriving from a 2-D electrode array, as a 1-D plus time signal. This transform speeds up and makes simpler the data analysis allowing, as said, the application of nonlinear signal processing techniques.

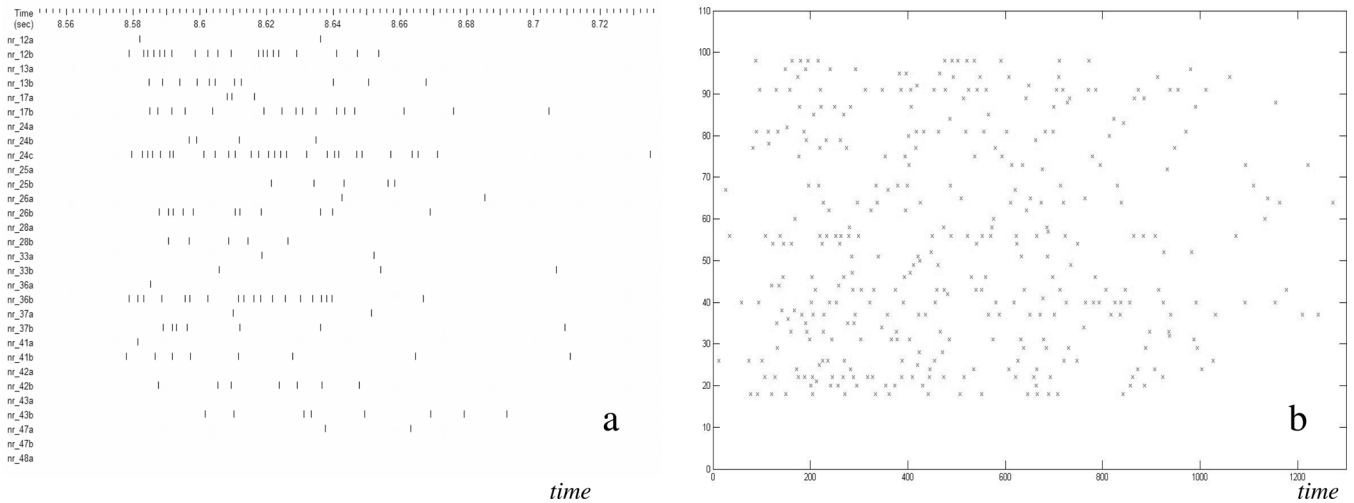


Fig. 3. Example of the projection obtained by the SAT on a real burst. (a) The raster plot of a real burst displayed thanks to the NeuroExplorer commercial software (Next Technologies, MA). On the  $x$  axis is reported the absolute time of the recording (seconds); on the  $y$  axis are listed the channel names. (b) The 1-D signal resulting from the SAT (displayed in Matlab7.0, The Mathworks, MA). On the  $x$  axis is reported the frame number of the burst (being 0-time the burst onset and 0.1 ms the interframe time, hence, e.g., 200 = 20 ms); on the  $y$  axis is the amplitude of the obtained SAT signal (arbitrary chosen between 100 and  $(100 - n)$ , being  $n$  the number of channels).

### C. Long-Term Correlation Estimation

A signal displaying a power law spectral density near the origin is called “one-over- $f$ ” noise. Such signals are commonly observed in many different systems, including physical, biological, physiological, economic, technological, and sociological ones [22]. In particular, many classical observations reported these kind of dynamics in neurophysiological signals, such as [18], [25]–[29]. When  $P(f) \approx 1/f^\alpha$ , with  $P(f)$  the signal power spectral density (PSD), for  $f \rightarrow 0$  and some  $\alpha > 0$ , it is often possible to define some sort of generalized correlation function (such as, e.g., the autocorrelation function) which is found to decay very slowly (hyperbolically).

The slow decay signifies that the current value of the series is affected not only by its most recent values but also by its past values. For this reason, such processes are often referred to as “long-memory” or “long-range dependence” processes [22]. In this specific case, we are interested in evaluating the presence of long-term correlations in the global activity of the neuronal network. The SAT signal, representing with no distortion the spatial and temporal information of the raster plot, is a very good candidate in showing long-term correlations.

As a matter of fact, other works report, while employing different methods, the presence of such a dynamics in neurophysiologic recordings (see, e.g., [19], [20], [30]).

Fig. 4 summarizes the different physical properties that long-term correlated signals exhibit as a function of the  $\alpha$  slope value their PSD assumes.  $\alpha$  near 0 indicates the presence of a stationary process with zero correlation, i.e., a white noise. An  $\alpha$  between 0 and 1 indicates a long-range positively correlated stationary signal. An  $\alpha$  between 1 and 2 indicates a long-range negatively correlated non-stationary signal and, finally, an  $\alpha$  between 2 and 3 indicates a long-range positively correlated non-stationary signal. If  $\alpha = 2$ , the process is classified as Brownian motion.

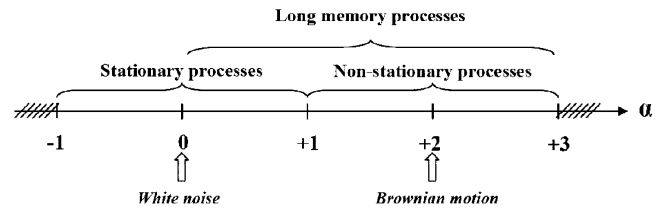


Fig. 4. Graphical representation of the physical meaning of the  $\alpha$  parameter.

We recall that, both white noise and Brownian motion signals are characterized by zero correlations among samples, but while white noise is a stationary signal (hence produces oscillations around a fix mean value), Brownian motion is a nonstationary signal, resulting in strong trends. One of the simplest method for the  $\alpha$  estimation is the log-periodogram regression, or simply, the periodogram analysis [22], [31], [32]. This method estimates  $\alpha$  as the linear slope of the periodogram (a discrete Fourier transform spectrum), in a log-log plot, close to the zero frequency axis. As a matter of fact, being  $P(f) \approx 1/f^\alpha$ , for  $f \rightarrow 0$  and some  $\alpha > 0$ ,  $\log(P(f)) \approx -\alpha \cdot \log(f)$ . Fig. 5 shows an example of the  $\alpha$  coefficient estimation in the periodogram of a burst taken from the experimental dataset (estimated on  $N = 400$  points). The range of periodogram plot regression was chosen in the two lowest decades of frequencies ( $2 \cdot 10^{-4} - 10^{-2}$  Hz), i.e., considering samples occurring from one to every 200 ms to one to every 10 ms, considering a sampling resolution of 0.1 ms. These values were chosen by considering as minimal frequency value (1 event over 200 ms) the maximal window length considered for a single burst (see Section II-B) and, as minimal value (1 event over 10 ms), a signal window that, on average, could contain at least 25 spikes (evaluated on the experimental dataset).

We applied the above described methods (burst detection, SAT, and Periodogram analysis) to 12 “dense” and 12 “small” longitudinal recordings from [17], ranging from the 6th to the 35th div. Each recording contained hundreds of bursts.

TABLE I  
AVERAGE  $\alpha$  TREND, REPRESENTED DIV BY DIV, OBTAINED AS AVERAGING OF ALL THE 12 “DENSE” CULTURES (TOP ROW) AND THE 12 “SMALL” CULTURES (BOTTOM ROW): avg  $\pm$  std

|              |       | Days in vitro |             |             |             |             |             |             |             |             |             |             |             |             |             |             |             |             |
|--------------|-------|---------------|-------------|-------------|-------------|-------------|-------------|-------------|-------------|-------------|-------------|-------------|-------------|-------------|-------------|-------------|-------------|-------------|
|              |       | 6             | 12          | 15          | 17          | 18          | 19          | 20          | 21          | 22          | 24          | 26          | 28          | 31          | 32          | 33          | 34          | 35          |
| <b>dense</b> |       | 0.275         | 0.330       | 0.625       | 1.553       | 1.529       | 1.681       | 1.597       | 1.672       | 1.597       | 1.697       | 2.010       | 1.952       | 2.163       | 1.962       | 1.967       | 2.039       | 1.996       |
|              | $\pm$ | $\pm$ 0.335   | $\pm$ 0.230 | $\pm$ 0.264 | $\pm$ 0.268 | $\pm$ 0.153 | $\pm$ 0.213 | $\pm$ 0.152 | $\pm$ 0.236 | $\pm$ 0.132 | $\pm$ 0.123 | $\pm$ 0.032 | $\pm$ 0.056 | $\pm$ 0.132 | $\pm$ 0.200 | $\pm$ 0.410 | $\pm$ 0.132 | $\pm$ 0.203 |
| <b>small</b> |       | 0.511         | 0.309       | 0.420       | 1.638       | 1.626       | 1.729       | 1.550       | 1.732       | 1.442       | 1.399       | 1.768       | 1.937       | 1.832       | 1.888       | 2.037       | 2.106       | 2.003       |
|              | $\pm$ | $\pm$ 0.218   | $\pm$ 0.217 | $\pm$ 0.122 | $\pm$ 0.257 | $\pm$ 0.223 | $\pm$ 0.201 | $\pm$ 0.199 | $\pm$ 0.276 | $\pm$ 0.206 | $\pm$ 0.184 | $\pm$ 0.168 | $\pm$ 0.103 | $\pm$ 0.177 | $\pm$ 0.164 | $\pm$ 0.284 | $\pm$ 0.234 | $\pm$ 0.159 |

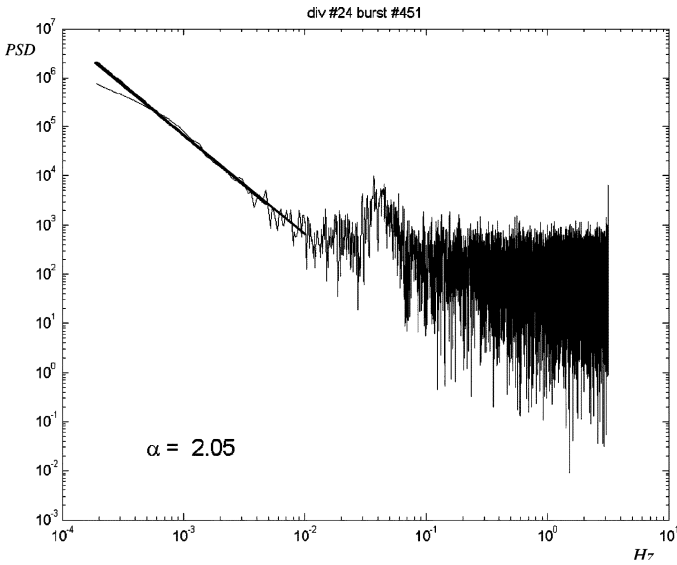


Fig. 5. Example of a  $\alpha$  estimation from a single 24-div burst Periodogram. The straight line represents the interpolation used for the estimation of the  $\alpha$  slope parameter. (Periodogram estimated on  $N = 400$  samples from  $2 \cdot 10^{-4} - 10^{-2}$  Hz). The same estimation is performed for all the bursts present in each one of the recordings.

III. RESULTS

We obtained 12 plots for each one of the two datasets (“dense” and “small”) showing, on the  $y$  axis, the mean  $\alpha$  value ( $\pm$ std) of all bursts versus the number of *days in vitro* (on the  $x$  axis). All plots showed a similar trend, exemplified in Fig. 6. The average trends, obtained as averaging of all the 12 cultures for the two populations, are reported in Table I. We found that the  $\alpha$  coefficient is close to 0.5 in the first two *weeks in vitro* (wiv) (indicating a positive long-term correlation in a nonstationary time series).  $\alpha$  suddenly grows to 1.5 circa around the 17th div ( $\pm 2$  div) and then irregularly grows till 2 in the following 20 days. The same trend is advisable in both the datasets.

IV. DISCUSSION

The behavior of the  $\alpha$  exponent across the culture development can be divided in three stages, which are well represented in Fig. 6. The first stage essentially coincides with the first two wiv. In this period  $\alpha$  is  $\leq 0.5$ , representing a condition in which the SAT signal is stationary (over the 200 ms long burst time window) and presents a positive correlation. It is known that in

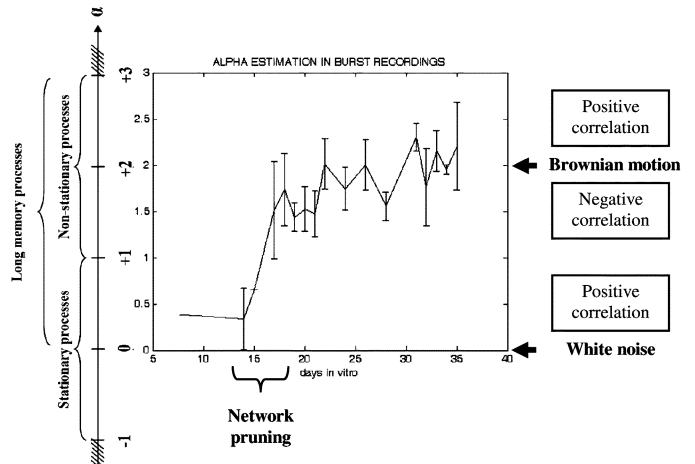


Fig. 6. An example of  $\alpha$  estimation results in a longitudinal “dense” rat cortical neuronal MEA recording. The  $x$  axis represents the number of day *in vitro* (div); the  $y$  axis shows the corresponding  $\alpha$  value. The scatter bars represent the  $\alpha$  variations (mean  $\pm$  std) among all the bursts that take place in a recording at a specific div.

the first one or two wiv the network is poorly bursting and the spiking activity can be classified as “global,” i.e., bursts usually involve almost the whole neuronal network [17], [33]–[35].

The presence of slow trends in the SAT-transformed signal that derives from the global structure of the activity, accounts for this topological characteristic.

The second stage is represented by a sudden change in the  $\alpha$  exponent around the 17th div. As known from literature, in a period comprised between the 6th and the 18th div, the network reorganizes its synaptic connectivity through a process called “pruning” [17], [34], [36], [37]. Through this remodeling, the network sacrifices useless synapses and optimizes neuronal links. At the same time, from the spiking activity viewpoint, the network begins to produce a higher number of bursts characterized by a localized activity (i.e., bursts involve a limited number of neurons). This is a typical sign of the creation of subnetworks [34], [37]. In this stage,  $\alpha$  suddenly raises to a value close to 1.5 and remains at this value for 2–8 div. Such an  $\alpha$  indicates the presence of a nonstationary signal with a strong negative correlation.

The presence of localized activity produces pronounced discontinuities in the SAT signal, confirming the signal as a nonstationary negatively correlated.

The last stage involves (at least) the 15 div following the previous stage. This period is characterized by a slow  $\alpha$  increment toward  $\alpha \approx 2$ . This condition corresponds to a nonstationary signal that exhibits a trend similar to a Brownian motion. This state testifies an energetically stable system and this is probably the reason why the activity in form of random oscillations can be observed in neuronal subnetworks [17].

These observations are supported by the morphological and temporal considerations obtained through the direct observation of regular bursts [17]. The same results were obtained by analyzing the less dense cultures classified as “small” in [17].

As it can be seen by comparing the presented results with literature, e.g., [19], [38], the proposed simple method it is able to obtain an estimation of the  $\alpha$  value identical to the one proposed by that authors ( $\alpha \approx 1.5$  for a mature network) but using a very limited burst population.

The request of a very small number of bursts allowed us to obtain an  $\alpha$  estimation also for the scarcely-bursting immature networks (less than 8 div) that is precluded to other methods. This allowed to observe, for the first time, the sudden  $\alpha$  value discontinuity presumably corresponding to the putative network pruning [36].

It is furthermore interesting to note that, while in various *in vivo* observations the  $\alpha$  coefficient is close to 1 [18], [27]–[29], in many cultured neurons studies the occurrence of this value is not statistically relevant (not in our work nor, e.g., in [19] and [21]). The situation  $\alpha = 1$  holds a central position in modern nonlinear signal processing theory because it is the hallmark of self-organized criticality (SOC) systems [39], [40]. SOC are systems composed by a multitude of oscillators (such as neurons) in which the dynamical attractors are critical points [39], [40]. This kind of system works in an energetically unstable condition, that lies at the “edge of a critical transition” (the “basal-activity-to-burst” transition in neuronal networks), that it is supposed to grant the best computational performance [41], [42]. It is possible that external modulations keep the *in vivo* systems in this energetically unstable condition that we are (at the moment) unable to reproduce in *in vitro* cultures. This could be the rationale of the sudden transition between the two very stable conditions of white noise ( $\alpha = 0$ ) and Brownian motion ( $\alpha = 2$ ) we noticed on culture recordings.

Finally, we point out that the kind of analysis we employed in this context seems to be able to highlight activity modifications that involve the whole neuronal network. The future development of our work is to show the usefulness of this kind of approach in analyzing other aspects of neuronal networks, e.g., in presence of chemical or electrical stimulation.

## V. CONCLUSION

The results presented in this work suggest a simple method for the analysis of the statistical characteristics of neuronal network activity. This approach has the advantage to use a well-standardized signal processing methods, such as periodogram, for finally obtaining a power-law fitting with the experimental data from the whole-network-activity. Previously, the whole-network-activity nonlinear analyses required the creation of *ad hoc* laborious and less repeatable methods.

Concerning the biological results, we were able to divide the network development in three stages. A first stage (between the

6th and the 16th div *circa*) was characterized by a signal stationarity together with a positive long-term correlation. The second stage, corresponding to the network pruning, was characterized by a sudden  $\alpha$  increment which indicates the nonstationarity of the signal endowed with a long-term correlation behavior characterized by negative correlations. This could be probably the consequence of subnetworks creation, which is typical of the development of self-assembling neuronal networks. Finally, network maturity was accompanied by a progressive  $\alpha$  increment toward  $\alpha \approx 2$ , i.e., toward a Brownian motion-like process. In general, this analysis suggests that networks spontaneously produce long-term correlated activity; a sudden transition between white-noise-like behavior and Brownian-motion-like behavior was noticed, while avoiding the energetically unstable condition  $\alpha = 1$ , typical of numerous *in vivo* recordings.

## ACKNOWLEDGMENT

The authors would like to thank J. Lamanna for the support in the creation and implementation of the analysis procedures. The authors would like to thank J. Pine and D. A. Wagenaar from the California Institute of Technology for providing MEA data described in [17].

## REFERENCES

- [1] M. Canepari, M. Bove, E. Maeda, M. Cappello, and A. Kawana, “Experimental analysis of neuronal dynamics in cultured cortical networks and transitions between different patterns of activity,” *Biol. Cybern.*, vol. 77, pp. 153–162, 1997.
- [2] M. H. Droge, G. W. Gross, M. H. Hightower, and L. E. Czisny, “Multielectrode analysis of coordinated, multisite, rhythmic bursting in cultured CNS monolayer networks,” *J. Neurosci.*, vol. 6, pp. 1583–1592, 1986.
- [3] D. G. Emery, J. H. Lucas, and G. W. Gross, “Contributions of sodium and chloride to ultrastructural damage after dendrotomy,” *Exp. Brain Res.*, vol. 86, pp. 60–72, 1991.
- [4] A. Harsch, K. Konno, H. Takayama, N. Kawai, and H. Robinson, “Effects of (alpha)-pompilidotoxin on synchronized firing in networks of rat cortical neurons,” *Neurosci. Lett.*, vol. 252, pp. 49–52, 1998.
- [5] Y. Jimbo, H. P. C. Robinson, and A. Kawana, “Strengthening of synchronized activity by tetanic stimulation in cortical cultures: Application of planar electrode,” *IEEE Trans. Biomed. Eng.*, vol. 45, no. 11, pp. 1297–1304, Nov. 1998.
- [6] E. W. Keefer, S. J. Norton, N. A. J. Boyle, V. Talesa, and G. W. Gross, “Acute toxicity screening of novel AChE inhibitors using neuronal networks on microelectrode arrays,” *Neurotoxicology*, vol. 22, pp. 3–12, 2001.
- [7] B. K. Rhoades, J. C. Weil, J. M. Kowalski, and G. W. Gross, “Distribution-free graphical and statistical analysis of serial dependence in neuronal spike trains,” *J. Neurosci. Methods*, vol. 64, pp. 25–37, 1996.
- [8] J. Streit, A. Tschertter, M. O. Heuschkel, and P. Renaud, “The generation of rhythmic activity in dissociated cultures of rat spinal cord,” *Eur. J. Neurosci.*, vol. 14, pp. 191–202, 2001.
- [9] G. G. Turrigiano, “Homeostatic plasticity in neuronal networks: The more things change, the more they stay the same,” *Trends Neurosci.*, vol. 22, pp. 221–227, 1999.
- [10] G. Zhu, M. Okada, T. Murakami, A. Kamata, Y. Kawata, K. Wada, and S. Kaneko, “Dysfunction of M-channel enhances propagation of neuronal excitability in rat hippocampus monitored by multielectrode dish and microdialysis systems,” *Neurosci. Lett.*, vol. 294, pp. 53–57, 2000.
- [11] A. M. M. C. Habets, A. M. J. Van Dongen, F. Van Huizen, and M. A. Corner, “Spontaneous neuronal firing patterns in fetal rat cortical networks during development in vitro: A quantitative analysis,” *Exp. Brain Res.*, vol. 69, pp. 43–52, 1987.
- [12] M. A. Corner and G. J. A. Ramakers, “Spontaneous bioelectric activity as both dependent and independent variable in cortical maturation: Chronic tetrodotoxin versus picrotoxin effects on spike-train patterns in developing rat neocortex neurons during long-term culture,” *Ann. NY Acad. Sci.*, vol. 627, pp. 349–353, 1991.
- [13] T. A. Basarsky, V. Parpura, and P. G. Haydon, “Hippocampal synaptogenesis in cell culture: Developmental time course of synapse formation, calcium influx, and synaptic protein distribution,” *J. Neurosci.*, vol. 14, pp. 6402–6411, 1994.

- [14] T. H. Murphy, L. A. Blatter, W. G. Wier, and J. M. Baraban, "Spontaneous synchronous synaptic calcium transients in cultured cortical neurons," *J. Neurosci.*, vol. 12, pp. 4834–4845, 1992.
- [15] H. Kamioka, E. Maeda, Y. Jimbo, H. P. C. Robinson, and A. Kawana, "Spontaneous periodic synchronized bursting during formation of mature patterns of connections in cortical cultures," *Neurosci. Lett.*, vol. 206, pp. 109–112, 1996.
- [16] R. Segev, Y. Shapira, M. Benveniste, and E. Ben-Jacob, "Observations and modeling of synchronized bursting in two-dimensional neural networks," *Phys. Rev. E, Stat., Nonlinear, Soft Matter Phys.*, vol. 64, p. 011920, 2001.
- [17] D. A. Wagenaar, J. Pine, and S. M. Potter, "An extremely rich repertoire of bursting patterns during the development of cortical cultures," *BMC Neurosci.*, vol. 7, p. 11, 2006.
- [18] M. C. Teich, C. Heneghan, S. B. Lowen, T. Ozaki, and E. Kaplan, "Fractal character of the neural spike train in the visual system of the cat," *J. Opt. Soc. Amer. A*, vol. 14, pp. 529–546, 1997.
- [19] J. M. Beggs and D. Plenz, "Neuronal avalanches in neocortical circuits," *J. Neurosci.*, vol. 23, p. 11167, 2003.
- [20] R. Segev, M. Benveniste, E. Hulata, N. Cohen, A. Palevski, E. Kapon, Y. Shapira, and E. Ben-Jacob, "Long term behavior of lithographically prepared in vitro neuronal networks," *Phys. Rev. Lett.*, vol. 88, p. 118102, 2002.
- [21] V. Pasquale, P. Massobrio, L. L. Bologna, M. Chiappalone, and S. Martinoia, "Self-organization and neuronal avalanches in networks of dissociated cortical neurons," *Neuroscience*, vol. 153, pp. 1354–1369, 2008.
- [22] J. Beran, *Statistics for Long-Memory Processes*. New York: Chapman & Hall/CRC, 1994.
- [23] D. A. Wagenaar, T. B. DeMarse, and S. M. Potter, "MeaBench: A toolset for multi-electrode data acquisition and on-line analysis," in *Proc. 2nd Int. IEEE-EMBC 2005*, 2005, pp. 518–521.
- [24] F. Esposti, J. Lamanna, and M. G. Signorini, "A new approach to the spatio-temporal pattern identification in neuronal multi-electrode registrations," in *Proc. Neurosci. Today, Firenze 2007*, 2005, pp. 21–24.
- [25] M. E. Wise, C. E. A. Taillie, Ed., "Spike interval distributions for neurons and random walks with drift to a fluctuating threshold," in *Statistical Distributions in Scientific Work*. Boston, MA: Reidel, 1981, vol. 6, pp. 211–231.
- [26] M. Kobayashi and T. Musha, "1/f fluctuation of heartbeat period," *IEEE Trans. Biomed. Eng.*, pp. 456–457, 1982.
- [27] F. Grüneis, M. Nakao, Y. Mizutani, M. Meesmann, and T. Musha, "Further study on 1/f fluctuations observed in central single neurons during REM sleep," *Biol. Cybern.*, vol. 68, pp. 193–198, 1993.
- [28] S. B. Lowen and M. C. Teich, "The periodogram and Allan variance reveal fractal exponents greater than unity in auditory-nerve spike trains," *J. Acoust. Soc. Amer.*, vol. 99, pp. 3585–3591, 1996.
- [29] M. C. Teich, R. G. Turcott, and R. M. Siegel, "Temporal correlation in cat striate-cortex neural spike trains," *IEEE Eng. Med. Biol. Mag.*, vol. 15, no. 5, pp. 79–87, Sep./Oct. 1996.
- [30] D. A. Wagenaar, Z. Nadasy, and S. M. Potter, "Persistent dynamic attractors in activity patterns of cultured neuronal networks," *Phys. Rev. E*, vol. 73, p. 51907, 2006.
- [31] P. Flandrin, "On the spectrum of fractional Brownian motions," *IEEE Trans. Inf. Theory*, vol. 35, no. 1, pp. 197–199, Jan. 1989.
- [32] M. S. Taqqu, V. Teverovsky, and W. Willinger, "Estimators for long-range dependence: An empirical study," *Fractals*, vol. 3, pp. 785–798, 1995.
- [33] E. Maeda, H. P. Robinson, and A. Kawana, "The mechanisms of generation and propagation of synchronized bursting in developing networks of cortical neurons," *J. Neurosci.*, vol. 15, pp. 6834–6845, 1995.
- [34] F. Esposti and M. G. Signorini, "Synchronization of neurons in micro-electrode array cultures," *Eur. Phys. J. Special Topics*, vol. 165, pp. 129–135, 2008.
- [35] F. Esposti, M. G. Signorini, J. Lamanna, F. Gullo, and E. Wanke, "How do TTX and AP5 affect the post-recovery neuronal network activity synchronization?," in *Proc. IEEE-EMBC Lyon 2007*, 2007, pp. 3012–3015.
- [36] O. Shefi, E. Ben-Jacob, and A. Ayali, "Growth morphology of two-dimensional insect neural networks," *Neurocomputing*, vol. 44, p. 635, 2002.
- [37] J. Van Pelt, P. S. Wolters, M. A. Corner, W. L. C. Rutten, and G. J. A. Ramakers, "Long-term characterization of firing dynamics of spontaneous bursts in cultured neural networks," *IEEE Trans. Biomed. Eng.*, vol. 51, no. 11, pp. 2051–2062, Nov. 2004.
- [38] C. V. Stewart and D. Plenz, "Homeostasis of neuronal avalanches during postnatal cortex development in vitro," *J. Neurosci. Methods*, vol. 169, pp. 405–416, Apr. 30, 2008.
- [39] P. Bak, C. Tang, and K. Wiesenfeld, "Self-organized criticality," *Phys. Rev. A*, vol. 38, pp. 364–374, 1988.

- [40] P. Bak, C. Tang, and K. Wiesenfeld, "Self-organized criticality: An explanation of the 1/f noise," *Phys. Rev. Lett.*, vol. 59, pp. 381–384, 1987.
- [41] H. J. Jensen, *Self-Organized Criticality: Emergent Complex Behavior in Physical and Biological Systems*. Cambridge, U.K.: Cambridge Univ. Press, 1998, p. 168.
- [42] O. Kinouchi and M. Copelli, "Optimal dynamical range of excitable networks at criticality," *Nature Phys.*, vol. 2, p. 348, 2006.



**Federico Esposti** (M'05) received the Ph.D. degree in biomedical engineering at the Politecnico di Milano, Milan, Italy, in 2009, focusing on the analysis of signals and images deriving from nervous systems. In particular, he developed different methods for the analysis of multi-electrode arrays and microscopic molecular imaging data.

At the moment, he is a Post-Doctoral Researcher at the Politecnico di Milano, Bioengineering Department and at the Medical Research Council Laboratory of Molecular Biology, Cambridge, U.K.



**Maria G. Signorini** received the Ph.D. degree in bioengineering from the Biomedical Engineering Department, Politecnico di Milano, Milan, Italy, in 1995.

She is Associate Professor at the Biomedical Engineering Department at the Politecnico di Milano, Italy. Her main research interests are nonlinear analysis and modeling of biological signals and systems regarding, in particular, cardiovascular and neuronal dynamics. She cooperates in industrial projects (HP Italy, Sister-Fresenius Medical Care) on biomedical

signal processing and instrumentation improvement. 2003 to date she is the Coordinator of the Ph.D. Program in Bioengineering.



**Steve M. Potter** received the B.S. degree in chemistry/biochemistry from the University of California, San Diego, and the Ph.D. degree in neurobiology from the University of California, Irvine, focusing on protein damage in calmodulin.

He is Associate Professor of Biomedical Engineering in the Laboratory for Neuroengineering at the Georgia Institute of Technology, Atlanta, since 2002. In the laboratory of Scott Fraser, he pioneered multiphoton microscopy, and vital GFP imaging. In the laboratory of Jerome Pine, he developed the

first closed-loop neuro-robotic systems for cultured neural networks, and new techniques for bi-directional MEA neural interfaces. He pioneered models for studying learning, memory, and neural dynamics *in vitro*, founding the field of embodied cultured networks.



**Sergio Cerutti** (M'81–S'97–F'02) is Professor on Biomedical Signal and Data Processing at the Bioengineering Department, Politecnico di Milano Italy where he was Chairman from 2000 to 2006. His research activity mainly concerns various aspects of biomedical signal processing and modelling related to the cardiovascular system and in the field of neurosciences. He is the author of more than 200 papers in indexed journals published in international scientific literature.

Prof. Cerutti is a Fellow Member of EAMBES and Associate Editor of IEEE TRANSACTIONS ON BIOMEDICAL ENGINEERING. During 1993–1996 he was Elected Member of IEEE-EMBS AdCom (Region 8) and he is Chairman of the IEEE-EMBS Technical Committee on Biomedical Signal Processing. He was the local organizer of four IEEE Summer Schools held in Siena. In 2009 he received the IEEE EMBS Academic Career Achievement Award.